

Link Budget Analysis for Secure Thermal Infrared Communications using Engineered Blackbody Radiation

Xiaoxin Liang^{1,2}, Fangjing Hu¹, Yuepeng Yan² and Stepan Lucyszyn^{1*}

¹Centre for Terahertz Science and Engineering and Department EEE, Imperial College London, Exhibition Road, London SW7 2AZ, UK.

²Institute of Microelectronics of Chinese Academy of Sciences, 3 Beitucheng West Road, Chaoyang District, Beijing 100029, PR China.

E-mail: s.lucyszyn@imperial.ac.uk

Abstract — The ‘THz Torch’ concept was recently introduced as an ultra-low cost means of providing secure short-range wireless communications in the thermal infrared spectral range (10-100 THz). This technology exploits engineered blackbody radiation, by partitioning thermally-generated spectral noise power into pre-defined frequency channels; the energy in each channel is then independently pulsed modulated and transmitted. This technology can be further enhanced by multiplexing schemes, e.g. frequency division multiplexing (FDM) and frequency-hopping spread-spectrum (FHSS). In this paper, the end-to-end link budget analysis for a 4-channel ‘THz Torch’ working demonstrator, operating over a short transmission range of 1 cm, is given for the first time. Mathematical modelling of the end-to-end wireless link is presented. In the analysis, different bias points for the source are considered and the corresponding RMS output voltages at the receivers are calculated. The predicted results show the capability for each channel, and will serve as a guide for further improving the overall performance of this multi-channel ‘THz Torch’ system.

Index Terms — THz Torch, wireless communications, thermal infrared, link budget, blackbody radiation.

I. INTRODUCTION

Terahertz (THz) systems are notoriously large and very expensive, from complete systems down to individual front-end active devices and passive components. Efforts are being made towards low-cost THz engineering, and demonstrators have been reported in recent years [1]. At present, there are no ubiquitous applications within in the terahertz frequency spectrum (from 0.3 to 10 THz). However, by moving into the high-THz part of the frequency spectrum (i.e. thermal infrared region, from 10 to 100 THz), for specific niche applications, it is possible to create affordable systems for commercial exploitation.

The thermal infrared (IR) frequency bands are best known for applications in thermography. There exists little in the way of enabling technologies in this part of the frequency spectrum to support wireless communications. This offers opportunities for developing secure communications within this largely unregulated part of the spectrum. The ‘THz Torch’ concept was recently presented as an ultra-low cost technology [2]–[6]. Single-channel links with a relatively low data rate of 380 bps has been reported [4]. Multi-channel ‘THz Torch’ systems using frequency division multiplexing (FDM) and frequency-

hopping spread-spectrum (FHSS) schemes have been proposed [3]. More recently, the first proof-of-concept multi-channel FHSS demonstrator was reported, and the integrity of both the FDM and FHSS systems to jamming and interception were evaluated in detail [5].

To quantitatively evaluate (in synthesis and analysis) the performance of this new wireless link technology, in an engineering context, link budget analysis is required. In this paper, and for the first time, we report the link budget analysis for thermal IR wireless communications based on engineered blackbody radiation. A 4-channel multiplexing system having a 320 bps data rate per channel is analyzed for a transmission range of 1 cm. The calculated results show the predicted performance for each channel within the pre-optimized working demonstrator [5].

II. SYSTEM OVERVIEW

The basic architecture for a single-channel ‘THz Torch’ link, without any collimating lenses, is shown in Fig. 1 [2]. With our setup, the transmitter consists of five incandescent light bulbs connected in series. The emitted output power is then filtered by a THz band pass filter (BPF) and the band-limited thermal noise power is modulated using ON-OFF keying (OOK). At the receiver end, the incoming energy is first filtered (by an identical THz filter as the one on the transmitter) and then detected and converted to an electrical signal by a pyroelectric (PIR) sensor. The received signal is then amplified and digitized by the post-processing circuitry, which contains a baseband low noise amplifier (LNA), baseband BPF and Schmitt trigger.

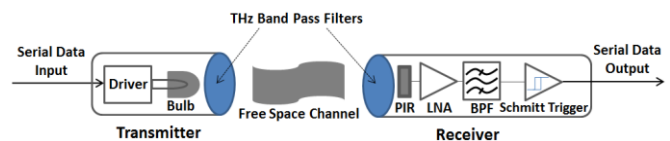


Fig. 1. Basic architecture for ultra-low cost ON-OFF keying ‘THz Torch’ wireless communications link [2].

The overall link budget breaks down into the transmitter, free space channel and receiver blocks, as shown in Fig. 2, where I_{filament} is the radiant intensity of the tungsten filament;

T_{GLASS} is the power transmittance of the bulb's glass envelope; $I_{primary}$ and $I_{secondary}$ are the radiant intensity from primary and secondary mechanism, respectively; T_{THz_BPF} is the power transmittance of the THz filter; I_{TX} is the total radiant intensity from the channel transmitter's source; L_{FS} is the free space loss; P_{RX} is the peak-to-peak power incident on the sensor; η_{PIR} is the responsivity of the sensor; A_{BB_LNA} is the voltage gain of the baseband LNA; A_{BB_BPF} is the voltage gain of the active baseband BPF; and V_{out} is the output RMS voltage at the receiver.

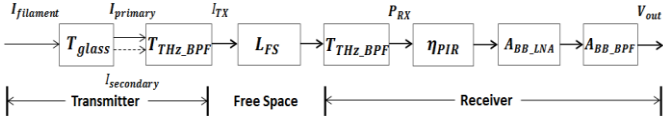


Fig. 2. Basic link budget representation for the thermal IR banded-noise wireless link.

III. LINK BUDGET ANALYSIS

The incandescent light bulb represents a convenient thermal IR noise source. For an ideal radiator (i.e. blackbody), its net spectral radiance can be calculated using Planck's law

$$I(\lambda, T) = \frac{2hc^2}{\lambda^5} \cdot \frac{1}{e^{hc/\lambda kT} - 1} - \frac{2hc^2}{\lambda^5} \cdot \frac{1}{e^{hc/\lambda kT_0} - 1} \quad (\text{W/m}^2/\text{sr}/\mu\text{m}) \quad (1)$$

where λ is the wavelength in free space; T is the absolute temperature of the radiator; T_0 is the absolute temperature of the ambient background; h is the Planck constant; c is the speed of light in vacuum; and k is the Boltzmann constant.

For non-ideal radiators, taking the effective radiating area and emissivity into account and then integrating over the spectral band of interest, the band-limited output radiant intensity can be expressed as

$$I(T) = A_{eff} \cdot \int_{\lambda_1}^{\lambda_2} \epsilon(\lambda, T) \cdot I(\lambda, T) d\lambda \quad (\text{W/sr}) \quad (2)$$

where A_{eff} is the effective area of the radiator, $\epsilon(\lambda, T)$ is the corresponding emissivity at λ and T , λ_1 and λ_2 are the lower and upper wavelengths of the spectral band of interest, respectively.

With our thermal noise source, the output radiant intensity can include both primary radiation from the tungsten filaments and secondary radiation from the glass envelopes. The radiant intensity from the primary radiation can be expressed as

$$I_{primary}(T_{filament}) = T_{GLASS} \cdot I_{filament}(T_{filament}) \quad (\text{W/sr}) \quad (3)$$

where T_{GLASS} can be obtained using measured data of the complex index of refraction for typical window glass [5, 6]; $A_{eff_filament}$ and $T_{filament}$ are the effective radiating area and temperature of the filaments, respectively.

The radiant intensity from secondary radiation can be calculated in a similar way. Instead of using an average glass temperature $T_{glass_average}$ for the source, for greater accuracy, it can be further divided into two regions; the cores (high

temperature, T_{glass_high}) and surrounding area (low temperature, T_{glass_low}).

The calculated bulb filament and measured glass envelope temperatures for different regions within the source, at different bias currents, are given in Table I. After channel filtering, $I_{TX}(T)$ represents contributions from both radiation mechanisms.

TABLE I

TEMPERATURES FOR FILAMENT AND GLASS ENVELOPE REGIONS

Temperature (K)	Bias current (mA)				
	44	50	60	70	80
Calculated $T_{filament}$	772	894	1042	1161	1262
Measured T_{glass_high}	312.3	318.9	331.8	346.9	366.1
Measured $T_{glass_average}$	306.3	310.6	319.9	330.9	344.9
Measured T_{glass_low}	306.0	310.4	319.4	330.4	344.2

Free space losses include spreading losses and atmospheric attenuation. If one considers the transmitter to be a point source, the free space loss can be calculated by

$$L_{FS} \approx T_{ATMOSPHERIC} \cdot \frac{A_s}{R^2} \cos \theta \quad (\text{sr}) \quad (4)$$

where $T_{ATMOSPHERIC}$ is the atmospheric transmittance within the channel, which is nearly 100% for a transmitter channel filter to receiver channel filter distance of 1 cm; $A_s = 9 \text{ mm}^2$ is the area of the sensing element; $R = 13.8 \text{ mm}$ is the total transmission distance from source to sensor; θ is zero in our case if perfect alignment is assumed.

At the receiver, the incident power $L_{FS} \cdot I_{TX}(T)$ passes through the matching channel filter, and absorbed by the sensor. The generated output voltage is then amplified and filtered by the post-processing circuit. The output RMS voltage $V_{out}(T)$ from each channel receiver can be estimated using

$$V_{out}(T) \approx \frac{A_{BB_BPF} \cdot A_{BB_LNA} \cdot \eta_{PIR}}{2\sqrt{2}} \cdot T_{THz_BPF} \cdot L_{FS} \cdot I_{TX}(T) \quad (\text{V}) \quad (5)$$

where η_{PIR} is the voltage responsivity of the detector, which is 5,850 V/W for the LME-553 sensor operating at 320 Hz [8], $A_{BB_LNA} = 99.4$ and $A_{BB_BPF} = 1.07$.

Predicted values for $V_{out}(T)$ are shown in Fig. 3, as a function of source bias current for the 4-channel multiplexing scheme working demonstrator described in [5]. It can be seen that Channel D exhibits the most significant voltage increase with biasing current. The reason is that Channel D is the nearest to the spectral radiance peak (which increases from 80 to 131 THz) of the primary radiation, and will benefit from the significant increase in band-limited output power. Similarly, Channel A benefits from the spectral radiance peak of the secondary radiation source, increasing from 31.7 to 35.6 THz, and from 32.3 to 37.9 THz, for low and high temperature regions respectively. Channel B is the least responsive, because it is far from the strong primary spectral radiance peak and not close enough to the weaker secondary spectral radiance peaks.

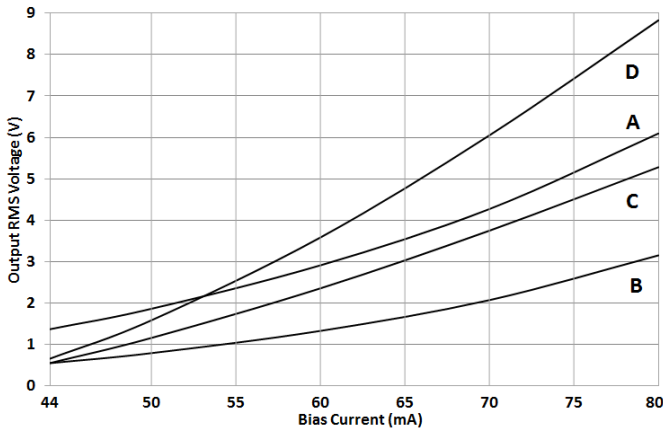


Fig. 3. Predicted receiver output RMS voltage from each channel (A: 15-34 THz; B: 42-57 THz; C: 60-72 THz and D: 75-89 THz) for different source bias currents, with the 4-channel multiplexing scheme working demonstrator described in [5].

IV. CONCLUSION

In this paper, an end-to-end link budget analysis for the thermal infrared banded-noise wireless communications link has been investigated for the first time. The output RMS voltages from each channel receiver in a multiplexed ‘THz Torch’ system have been calculated. It was found that the predicted results shown in Fig. 3 are very close to the measured values. In the basic link budget analysis given here, a number of assumptions have had to be made. Nevertheless, the results from this link budget analysis accurately predicts the channel behavior and channel-to-channel variations for a wireless systems that is based on thermodynamic front-end hardware in both eth transmitter and receiver. As a result, this analysis provides a valuable engineering tool, enabling system optimization or fault diagnosis to be performed.

ACKNOWLEDGEMENT

This work was partially supported by the China Scholarship Council (CSC).

REFERENCES

- [1] S. Lucyszyn, F. Hu and W. J. Otter, “Technology demonstrators for low-cost terahertz engineering,” *2013 IEEE Asia-Pacific Microwave Conference (APMC 2013)*, pp. 518-520, Nov. 2013.
- [2] S. Lucyszyn, H. Lu, and F. Hu, “Ultra-low cost THz short-range wireless link,” *2011 IEEE MTT-S International Microwave Workshop Series on Millimeter Wave Integration Technologies*, pp. 49-52, Sep. 2011.
- [3] F. Hu and S. Lucyszyn, “Ultra-low cost ubiquitous THz security systems,” *2011 IEEE Asia-Pacific Microwave Conference (APMC 2011)*, pp. 60-62, Dec. 2011.
- [4] F. Hu and S. Lucyszyn, “Improved ‘THz Torch’ technology for short-range wireless data transfer,” *2013 IEEE International Wireless Symp (IWS 2013)*, pp. 1-4, Apr. 2013.
- [5] X. Liang, F. Hu, Y. Yan and S. Lucyszyn, “Secure thermal infrared communications using engineered blackbody radiation,” *Scientific Reports*, Nature Publishing Group, Jun. 2014.
- [6] F. Hu and S. Lucyszyn, “Emerging thermal infrared ‘THz Torch’ technology for low-cost security and defence applications”, Chapter 13, pp. 239-275, “THz and Security Applications: *Detectors, Sources and Associated Electronics for THz Applications*”, NATO Science for Peace and Security Series B: Physics and Biophysics, C. Corsi and F. Sizov (Editors), Springer Netherlands, Apr. 2014
- [7] Northumbria Optical Coatings Ltd. Online catalogue. <http://www.noc-ltd.com/catalogue> (2011).
- [8] InfraTec, <http://www.infratec-infrared.com/Data/LME-553.pdf>